Sequence swapping does not result in conformation swapping for the β4/β5 and β8/β9 β-hairpin turns in human acidic fibroblast growth factor

JAEWON KIM, JIHUN LEE, STEPHEN R. BRYCH, TIMOTHY M. LOGAN, AND MICHAEL BLABER

Kasha Institute of Molecular Biophysics and Department of Chemistry and Biochemistry, Florida State University, Tallahassee, Florida 32306-4380, USA

Abstract

The β-turn is the most common type of nonrepetitive structure in globular proteins, comprising ~25% of all residues; however, a detailed understanding of effects of specific residues upon β-turn stability and conformation is lacking. Human acidic fibroblast growth factor (FGF-1) is a member of the β-trefoil superfold and contains a total of five β-hairpin structures (antiparallel β-sheets connected by a reverse turn). β-Turns related by the characteristic threefold structural symmetry of this superfold exhibit different primary structures, and in some cases, different secondary structures. As such, they represent a useful system with which to study the role that turn sequences play in determining structure, stability, and folding of the protein. Two turns related by the threefold structural symmetry, the β4/β5 and β8/β9 turns, were subjected to both sequence-swapping and poly-glycine substitution mutations, and the effects upon stability, folding, and structure were investigated. In the wild-type protein these turns are of identical length, but exhibit different conformations. These conformations were observed to be retained during sequence-swapping and glycine substitution mutagenesis. The results indicate that the β-turn structure at these positions is not determined by the turn sequence. Structural analysis suggests that residues flanking the turn are a primary structural determinant of the conformation within the turn.

Keywords: β-hairpin; fibroblast growth factor; folding kinetics; stability; turn conformation

Different types of secondary structures are recognized in proteins: helix, sheet, turns, and loops. Among these, turns and loops have received the least attention due to wide conformational variability and lack of simple model systems. Several successfully designed β-hairpins have been reported, including monomeric β-hairpins (Stanger and Gellman 1998; de Alba et al. 1999a) and turns associated with a three-stranded antiparallel β-sheet (Kortemme et al. 1998; Schenck and Gellman 1998; de Alba et al. 1999b). With these model systems, a close relationship was observed between turn stability and turn sequence. Furthermore, the effects of different amino acids, at specific locations within particular types of β-turns, upon stability and folding are being elucidated (Gibbs et al. 2002; Blandl et al. 2003; Kim et al. 2003; Rotondi and Gierasch 2003). However, more than 50% of turns have at least one residue in common with related turn types (Hutchinson and Thornton 1994); thus, the larger structural context within which turn sequences exist appears to be key to understanding their effects upon structure, thermodynamics, and folding kinetics.

Figure 1. (*Upper* panel) Relaxed stereo-ribbon diagram of FGF-1 (view looking down the threefold axis of tertiary structure symmetry) and showing the locations of the β-strands comprising the β4/β5 (gray) and β8/β9 (dark gray) β-hairpin turns. The locations of the N and C termini are also indicated. (*Lower* panel) Primary structure of FGF-1 (single-letter code) aligned according to the threefold tertiary structure symmetry and indicating the locations of the β4, β5, β8, and β9 β-strands.

Human acidic fibroblast growth factor (FGF-1) has a total of 12 β-strands, forming a series of five β-hairpin structures characteristic of the β-trefoil superfold (Fig. 1; Murzin et al. 1992; Orengo et al. 1994). Among these five turns, β4/β5 (i.e., connecting β-strands 4 and 5) and β8/β9 are related by the threefold tertiary structure symmetry inherent in the β-trefoil architecture. Turn β4/β5 has been argued to contribute to different binding specificities of FGF homologous factors (Olsen et al. 2003). This turn in FGF-1 has two overlapping conformations: a type IV turn (an approximate 180° turn in the main chain direction, but residues i+1 and i+2 within the turn do not exhibit characteristic φ, ψ angles) spanning residue positions 48–51 (i.e., residues i through i+3 of the turn) and a type II turn (i+1 φ ~−60° ψ ~+120°, i+2 φ ~+90° ψ ~0°) spanning residue positions 50–53 (Hutchinson and Thornton 1996). However, based on the crystal structure (Blaber et al. 1996) residue positions 49–52 within turn β4/β5 correspond to residues 90–93 within turn β8/β9 (Fig. 2). In this regard, there are no insertions or deletions when comparing the main chain regions that comprise turns β4/β5 and β8/β9, yet these turns exhibit significantly different turn conformations. Residue positions 90–93 in turn β8/β9 are defined as a type I turn (type I β-turn plus G1-type β-bulge; i+1 φ ~−60° ψ ~−30°, i+2 φ ~−90° ψ ~0°). The importance of this particular turn upon the protein stability and function has been discussed in several reports. An extensive contact between turn β8/β9 and fibroblast growth factor receptor (FGFR) has been described (Pellegrini et al. 2000). Alternate conformations for the β8/β9 turn have been reported, and have been proposed as a possible basis of various functionalities (Hecht et al. 2001; Fernandez-Tornero et al. 2003); however, a type I turn con-

formation for this region appears to be adopted in the absence of ligand interactions or crystal packing influences (Kim et al. 2002).

Turns β4/β5 and β8/β9 have different primary structures within the structurally heterogeneous region (S50, V51, G52 in turn β4/β5, and E91, N92, H93 in turn β8/β9) (Fig. 1), and an important question is whether the different turn conformations are a consequence of the heterogeneous primary structures within these regions. Furthermore, do the
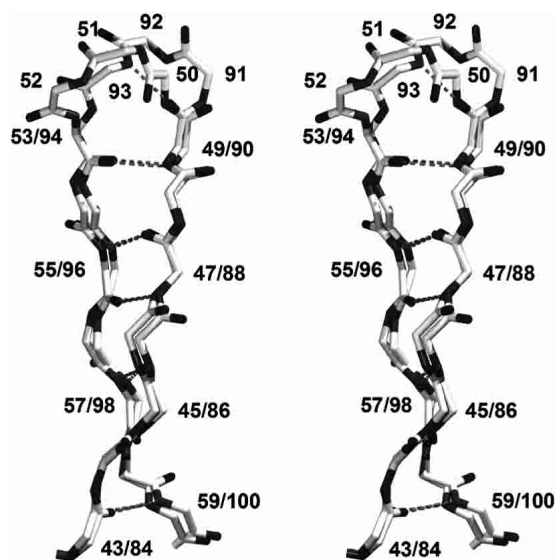
Figure 2. Relaxed stereo diagram of an overlay of the β4/β5 and β8/β9 turn regions. For purposes of clarity, only the main chain atoms are shown. The hydrogen bond interactions between the adjacent β-strands are also indicated.

different turn conformations exert differential contributions toward the stability and folding of the protein? In an attempt to answer these questions, we constructed a series of mutations designed to exchange the primary structures of both turns. Furthermore, we also constructed a series of glycine mutations within these turn regions to evaluate the nature of strain inherent within the turns. Folding kinetics, stability studies, and X-ray crystallographic and NMR analyses were used to quantify the effects of these mutations. The results indicate that the residues within the turns are not the primary determinant of the turn structure, but do have a significant influence on protein stability and folding. The primary determinants of the turn structure reside within the local environment, and in particular, are postulated to involve residue positions that flank the turns.

Results

Substitution of the β8/β9 turn primary structure into the β4/β5 turn

Mutations were constructed that stepwise substituted the β8/β9 turn primary structure into the β4/β5 turn, including V51N and G52H point mutants, S50E/V51N double mutant, and S50E/V51N/G52H triple mutant. The V51N point mutant and the S50E/V51N double mutant had no effect on protein stability (Table 1) or folding kinetics (Table 2). However, the G52H point mutation destabilized the protein by 5.5 kJ/mol, essentially due to a fourfold reduction in the folding rate (Table 2). The S50E/V51N/G52H triple mutant destabilized the protein by 3.6 kJ/mol, again, primarily due to a decrease (approximately twofold) in the rate of folding.

Substitution of the β4/β5 turn primary structure into the β8/β9 turn

Mutations were constructed that stepwise substituted the β4/β5 turn primary structure into the β8/β9 turn, including

Table 1. *Thermodynamic parameters for WT FGF-1 and mutant proteins determined from isothermal equilibrium denaturation*

Protein	ΔG_0 (kJ/mol)	*m*-value (kJ/mol M)	C_m (M)	$\Delta\Delta G^a$ (kJ/mol)
Wild type	21.1 ± 0.6	18.9 ± 0.6	1.11 ± 0.01	–
S50G/V51G	22.9 ± 0.1	19.4 ± 0.1	1.18 ± 0.01	−1.3
H93G	28.6 ± 0.2	19.8 ± 0.1	1.45 ± 0.01	−6.6
E91G/N92G/H93G	25.9 ± 0.3	21.0 ± 0.3	1.24 ± 0.01	−2.6
V51N	23.5 ± 0.2	21.0 ± 0.4	1.12 ± 0.01	−0.2
G52H	17.2 ± 1.1	20.7 ± 1.0	0.83 ± 0.02	5.5
S50E/V51N	21.5 ± 0.5	19.7 ± 0.8	1.09 ± 0.02	0.4
S50E/V51N/G52H	19.1 ± 0.1	20.6 ± 0.4	0.93 ± 0.02	3.6
E91S/N92V	18.0 ± 0.2	21.8 ± 0.1	0.83 ± 0.01	5.7
E91S/N92V/H93G	19.8 ± 1.2	20.4 ± 0.6	0.97 ± 0.01	2.8

[a] $\Delta\Delta G = (C_{m \ wild \ type} − C_{m \ mutant}) * (m_{wild \ type} + m_{mutant})/2$ (Pace and Scholtz 1997). A negative value for $\Delta\Delta G$ indicates a more stable mutant. All errors are listed as standard error of multiple data sets.

Table 2. *Folding and unfolding kinetic parameters for WT FGF-1 and mutant proteins*

Protein	k_f (sec^{-1})	m_f (M^{-1})	k_u (1 × 10^{-4}s^{-1})	m_u (M^{-1})
Wild type	3.75	−6.61	8.09	0.47
S50G/V51G	4.34	−6.43	7.71	0.50
H93G	55.05	−7.43	4.39	0.47
E91G/N92G/H93G	6.51	−6.17	7.80	0.54
V51N	3.47	−6.17	9.10	0.46
G52H	0.91	−5.96	9.41	0.45
S50E/V51N	4.03	−6.20	9.00	0.48
S50E/V51N/G52H	2.05	−7.14	9.97	0.39
E91S/N92V	0.77	−5.83	22.69	0.42
E91S/N92V/H93G	3.08	−6.69	15.37	0.35

a previously described H93G point mutant (Kim et al. 2002), an E91S/N92V double mutant, and an E91S/N92V/H93G triple mutant. The E91S/N92V double mutant destabilized the protein by 5.7 kJ/mol (Table 1). This destabilizing effect is due to both a fivefold reduction in the rate of folding and a threefold increase in the rate of unfolding (Table 2). The E91S/N92V/H93G triple mutant destabilized the protein by 2.8 kJ/mol, and is due primarily to a twofold increase in the rate of unfolding with only a slight decrease in the rate of folding (Table 2). Relative to the H93G mutant, the triple mutant E91S/N92V/H93G was destabilized by a substantial 9.6 kJ/mol, due to both an 18-fold reduction in the rate of folding and an approximately fourfold increase in the rate of unfolding (Table 2).

Glycine substitutions in the β4/β5 and β8/β9 turn regions

Three different combination glycine mutations (E49G, S50G/V51G, and E49G/S50G/V51G) were created within the β4/β5 turn. All three mutants were marginally more stable than the wild-type protein, with $\Delta\Delta G$ values ranging from −0.4 to −1.3 kJ/mol (Table 1). The unfolding rate for all three mutants was essentially unaffected, and the observed modest increases in stability are due primarily to increases in the rate of folding (Table 2). In reference to the G52H background, the introduction of glycine residues at positions 50 and 51 resulted in a slight increase in stability of −2.1 kJ/mol, due primarily to a twofold increase in the rate of folding. E91G, N92G, and H93G point mutations as well as an E91G/N92G double mutant in FGF-1 were characterized as part of a prior study of the β8/β9 loop region (Kim et al. 2002), and a combination triple glycine mutation, E91G/N92G/H93G, is reported here. The introduction of three glycine substitutions in the β8/β9 turn resulted in an increase in stability of −2.6 kJ/mol in comparison to the wild-type protein. As with the glycine mutations in the β4/β5 turn, this increase in stability is due almost exclusively

to an increase in the rate of folding, while the rate of unfolding is largely unaffected.

X-ray structure determinations

The V51N point mutation, S50G/V51G double mutant, and S50E/V51N double mutant yielded diffraction quality crystals, each in space group C222$_1$, and produced high-resolution data sets with good completion (Table 3). Each structure refined to similar values of R$_{free}$ (21.4%–22.7%) and R$_{cryst}$ (18.5%–19.7%) and with appropriate stereochemistry. The 2F$_o$ – F$_c$ difference electron density was unambiguous at the mutation site(s), and the mutant structures could be accurately modeled in each case.

NMR analysis

The backbone HN, N, CA, CB, and CO resonances of wild-type FGF were assigned (with the exception of residue E81) from correlations obtained in triple resonance NMR spectra, and are in excellent agreement with previous reports (Pineda-Lucena et al. 1994; Ogura et al. 1999). The wild-type assignments were used to guide the backbone assignments for the E91S/N92V/H93G triple mutant, and assignments were obtained for all residues except E81, Y74, and Y94. Figure 3 compares the backbone HN-HN NOE pattern obtained in a 3D ^{15}N-separated NOESY-HSQC spectrum for the residues found in the β4/β5 and β8/β9 turns within the E91S/N92V/H93G triple mutant. The NOE cross-peaks between residues 52 and 53, combined with the lack of cross-peaks between residues 51 and 52, are consistent with a type II turn for residue positions 50–53 (as identified from the X-ray structure [Blaber et al. 1996]). Despite the sequence identity within the β8/β9 turn region for the E91S/N92V/H93G triple mutant, the NOE cross-peaks between residues 91 and 92 and between 92 and 93 confirm a type I turn for residue positions 90–93 (identical to the wild-type β8/β9 turn).

Discussion

While the residues comprising the β4/β5 and β8/β9 turn regions (i.e., positions 50–52 and 91–93, respectively) differ in conformation, the adjacent β-sheet residues (43–49, 53–59 and 84–90, 94–100) exhibit a high degree of structural identity, and the main chain atoms overlay with an r.m.s. deviation of 0.6 Å (Fig. 2). The substitution of the β4/β5 turn primary structure into the β8/β9 turn, and the converse substitution of the β8/β9 turn primary structure into the β4/β5 turn, were observed to destabilize the protein in both cases. The degree of destabilization was of similar magnitude (2.8 and 3.6 kJ/mol, respectively), although it was achieved by differential effects on folding and unfolding rates (i.e., the mutation of the β4/β5 turn destabilized primarily through a decrease in the folding rate, whereas the mutation of the β8/β9 turn destabilized primarily through an increase in the unfolding rate). These results indicate that the primary structure within these turns, in both cases, is optimized to interact with the local structural environment.

Table 3. *Crystallographic data collection and refinement statistics*

	Wild type[a]	V51N	S50G/V51G	S50E/V51N
		Crystal data		
Space group	C222$_1$	C222$_1$	C222$_1$	C222$_1$
a (Å)	74.1	74.8	74.9	74.4
b (Å)	96.8	96.8	97.0	96.3
c (Å)	109.0	108.0	108.0	109.1
Matthews' coefficient	2.96	2.96	2.97	2.96
Max resolution (Å)	1.65	2.00	2.05	1.80
		Data collection and processing		
Total/unique reflections		334,966/26,820	330,387/25,055	145,475/36,350
% completion		99.9	99.9	99.0
% completion (highest shell)		99.9	100.0	95.1
I/σ (overall)		35.6	30.0	21.6
I/σ (highest shell)		4.3	3.6	2.2
Wilson B (Å)		12.8	11.9	9.7
R merge (%)		5.9	7.9	5.8
		Refinement		
R$_{cryst}$ (%)		19.0	19.7	18.5
R$_{free}$ (%)		22.7	22.7	21.4
R.M.S. bond length deviation (°)		0.008	0.007	0.008
R.M.S. bond angle deviation (°)		1.5	1.5	1.5
PDB accession		1PZZ	1Q03	1Q04

[a] Brych et al. 2001.
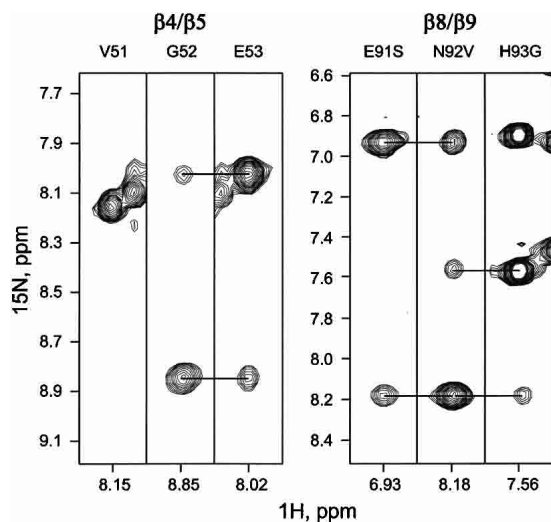
Figure 3. A composite plot of several slices taken from the 3D 15N-separated NOESY-HSQC spectrum of the E91S/N92V/H93G triple mutant. The *left* panel shows the HN-HN NOEs observed for residues V51-G52-G53 of turn β4/β5; the *right* panel shows the HN-HN NOEs observed for residues E91S-N92V-H93G in turn β8/β9. The lines indicate the location of sequential NOEs observed for each residue. The NOE cross-peaks between residues 52 and 53, combined with the lack of cross-peaks between residues 51 and 52, are consistent with a type II turn for residue positions 50–53. Despite the sequence identity within the β8/β9 turn region for the E91S/N92V/H93G triple mutant, the NOE cross-peaks between residues 91 and 92, and between 92 and 93, confirm a type I turn for residue positions 90–93.

Given that the β4/β5 and β8/β9 turn regions exhibit different conformations in the wild-type protein, an important question is whether the swapping of primary structure within these turns results in a corresponding conformational change. A crystal structure was obtained for the S50E/V51N double mutant that converts the *i*+1 and *i*+2 residues within the β4/β5 turn to the equivalent β8/β9 primary structure. These mutations resulted in no significant structural change to the β4/β5 turn (Fig. 4). The H93G point mutation structure was reported previously (Kim et al. 2002), and results in no conformational change to the β8/β9 turn. Thus, the same sequence E(*i*+1), N(*i*+2), and G(*i*+3) introduced into the β4/β5 turn adopts the characteristic overlapping type IV and type II turns, but when introduced into the β8/β9 turn adopts the characteristic type I turn. NMR spectra were used to further analyze the conformation of the β8/β9 turn with the E91S/N92V/H93G triple mutant (i.e., introducing the β4/β5 primary structure into the β8/β9 turn). An observed intense NOE between residue 91 (*i*+1) and 92 (*i*+2) eliminates the possibility that the β8/β9 turn adopts a type II or type II′ conformation. Likewise, an observed intense NOE between 92 (*i*+2) and 93 (*i*+3) eliminates the possibility that a type I′ is formed in the β8/β9 turn. Thus, this finding is consistent with the interpretation that the β4/β5 sequence introduced into the β8/β9 turn did not result in a conversion

to the β4/β5 turn conformation. Although we were unable to obtain structural data for the S50E/V51N/G52H triple mutant, the available data show that swapping the amino acid sequence of the β4/β5 and β8/β9 turns does not concomitantly convert the turn conformations. Therefore, we conclude that the local environment influences both the stability and the conformation of the β4/β5 and β8/β9 turns.

Glycine substitutions within ordered regions of a protein can destabilize the structure due to an increased entropy of unfolding (Matthews et al. 1987). However, such substitutions at turn positions known to fall outside the preferred positions of the Ramachandran plot can result in an increase in stability (due to the reduction in structural strain associated with eclipsed main chain/main chain and main chain/C^β groups) (Hutchinson and Thornton 1994; Kwasigroch et al. 1996; Takano et al. 2001; Kim et al. 2003). The S50G/V51G double mutant and E91G/N92G/H93G triple mutant both resulted in a modest stabilization of the protein (−1.3 and −2.6 kJ/mol, respectively). Thus, a polyglycine sequence in both turns can effectively substitute for the wild-type sequence (position 52 in the β4/β5 turn is glycine in the wild-type protein). However, despite the similar overall stability effects of such a substitution, there appear to be notable differences in these turn regions with regard to structural strain.

A comparison of the wild-type protein with the S50G/V51G double mutant, and similarly, a comparison of the H93G point mutant with the E91G/N92G/H93G triple mutant, evaluates the effect of glycine mutations at the *i*+1 and *i*+2 positions within the β4/β5 and β8/β9 turns when the *i*+3 position is a glycine. In the case of the β4/β5 turn, the conversion of the *i*+1 and *i*+2 positions to glycine results in a modest stabilization of −1.3 kJ/mol, and does not result in any structural changes within the turn region (Fig. 4). In the case of the β8/β9 turn, the conversion of the *i*+1 and *i*+2
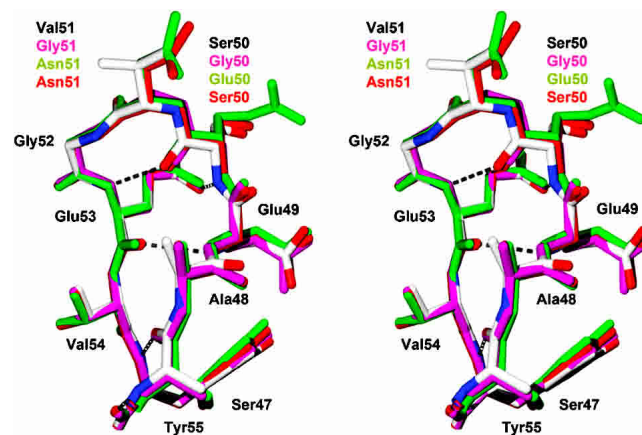
Figure 4. Relaxed stereo diagram illustrating an overlay of the β4/β5 turn regions for WT* (CPK coloring), V51N (red), S50G/V51G (magenta), and S50E/V51N (green) mutants. None of the sequence substitution, or polyglycine substitutions, within this turn affected the structure of the turn.

positions to glycine results in a significant destabilization of +4.0 kJ/mol (Table 1). A comparison of the H93G and G52H point mutations (i.e., comparing the effects of glycine vs. histidine at the $i+3$ position within the β4/β5 and β8/β9 turn regions) yields relatively consistent results for both turns, namely a destabilization of 5.5 to 6.6 kJ/mol upon the introduction of a histidine for glycine at this position. Thus, the β8/β9 turn $i+3$ histidine exhibits significant structural strain (being located in the left-handed α-helical region of the Ramachandran plot) (Kim et al. 2002), whereas the glycine residue at this symmetry-related position in the β4/β5 turn does not. Conversely, the $i+1$ and $i+2$ residues in the β8/β9 turn actively contribute to the stability of the structure (which is destabilized when converted to glycine), whereas similar positions in the β4/β5 turn do not. These results identify a fundamental difference between these two turns: the β4/β5 turn appears generally optimized and to have limited strain associated with it, whereas the β8/β9 turn exhibits an inherent structural strain, and can be further optimized to substantially (i.e., ~6.6 kJ/mol) increase protein stability. Thus, while a simple poly-glycine substitution within both turn regions can be accommodated, additional stability is achievable with an appropriate selection of side chains (e.g., E91/N92/G93 in the β8/β9 turn region).

What structural features outside of the immediate turns might be responsible for influencing the structure of the turns? An examination of an overlay of the β4/β5 and β8/β9 turn regions provides some possible answers. If the β8/β9 turn adopted the β4/β5 turn structure, it would result in a 2.9 Å close contact between the main chain carbonyl oxygen of position E91 (equivalent to S50) and the side chain L89 $C^{\delta 1}$ atom (Fig. 5). Associated with this contact is the hydrogen-bonding requirement of the main chain carbonyl group of E91, which could not be satisfied by such an interaction; thus, this conformation appears unfavorable. A more egregious close contact would occur if the β4/β5 turn adopted the β8/β9 turn structure. In this case an ~0.5 Å contact would occur between a side chain C^{γ} atom of V51 (equivalent to N92) and the side chain $O^{\varepsilon 1}$ atom of E53 (which is involved in a salt bridge with adjacent K100) (Fig. 5). The above interactions involve residues in the primary structure that are adjacent to the turn residues (i.e., positions 48/89 and 53/94); thus, the conformation of the residues within the turns appears to be determined not by the primary structure of the turn residues, but rather by the residues flanking the turns. In this regard, the main chain atom overlay of the two turns (Fig. 2) indicates that the structural deviations initiate with the ψ angles of residue positions 49 and 90, and extend through the φ angles of residues 53 and 94. These different main chain φ,ψ angles may dictate the observed structural difference within the two turns; however, since the residues at these positions are neither proline or glycine, the differences in main chain angles must be due to side chain interactions. Again, the results suggest that such interactions do not involve the side chains within the immediate turn region.
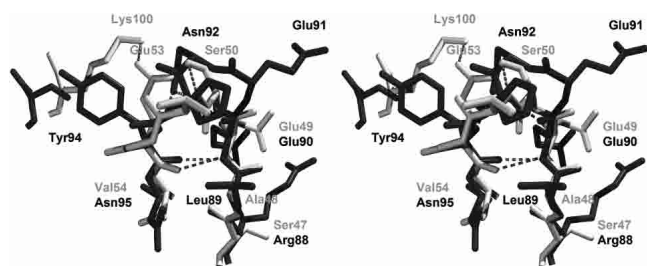
Despite the importance of β-hairpin structures in proteins, the principles underlying their formation and stability are not well understood. There are two different views regarding the contributions of residues within turn regions upon conformation. One view is that turn residues can determine the turn conformation (de Alba et al. 1997). The other view is that turn regions in a protein may be able to maintain their conformation despite variations in their primary structure (Searle et al. 1995). Several groups have examined the influence of turn sequences on the formation and stability of β-hairpins (Ramirez-Alvarado et al. 1997; Blanco et al. 1998; de Alba et al. 1999b; Griffiths-Jones et al. 1999; Chen et al. 2001). However, these studies used relatively small peptides, and the effects of adjacent regions outside of the turn (as would be present in larger globular proteins) could not be determined. In the present study, involving two symmetry-related turns within FGF-1, the data indicate that neither glycine substitution, nor sequence swapping, affected the local turn conformation. Furthermore, structural analysis suggests a role for flanking residues in determination of the turn conformation. These results support the general hypothesis of Searle et al. (1995) with regard to turn sequences and structures within proteins. Thus, predicting the stability and structure of turn regions within proteins requires knowledge of the larger structural context. However, the results suggest that a simple polyglycine primary structure will suffice for mesophilic applications. Finally, the results show that symmetry-related turn regions within a symmetric superfold can exhibit substantially different properties with regard to strain and contributions to overall folding kinetics.

Figure 5. Relaxed stereo diagram of a close-up of an overlay of the β4/β5 (light gray) and β8/β9 (dark gray) turns showing the local side chain interactions.

Materials and methods

Mutagenesis and expression

All studies utilized a synthetic gene for the 140-amino-acid form of human FGF-1 (Gimenez-Gallego et al. 1986; Linemeyer et al. 1990; Ortega et al. 1991; Blaber et al. 1996) with the addition of

an amino-terminal six-His tag to facilitate purification (Brych et al. 2001). The QuikChange site-directed mutagenesis protocol (Stratagene) was used to introduce all point mutations, and all mutations were confirmed by nucleic acid sequence analysis (Biomolecular Analysis Synthesis and Sequencing Laboratory, Florida State University). Mutant nomenclature utilizes the single-letter amino acid code (e.g., H93G refers to a glycine substitution for a histidine residue at position 93). All expression and purification followed previously published procedures (Brych et al. 2001). Purified protein was exchanged into 20 mM N-(2-acetamido)iminodiacetic acid (ADA), 100 mM NaCl, 2 mM DTT (pH 6.60) ("ADA buffer") for biophysical studies.

Isothermal equilibration denaturation

Protein samples (40–10 μM) in various concentrations of GuHCl/ADA buffer were allowed to equilibrate overnight at room temperature (298 K). This study made use of the fluorescence signal of the single endogenous tryptophan residue at position 107. This residue is ~90% buried in the native structure (Blaber et al. 1996). Complete details of the instrumentation, data collection, and analysis procedure were reported (Blaber et al. 1999). Briefly, the fluorescence signal of FGF-1 is atypical in that W107 exhibits greater quenching in the native state rather than the denatured state. Excitation at 295 nm provides selective excitation of W107 in comparison with the six tyrosine residues that are present in the structure (Blaber et al. 1999; Brych et al. 2001). Triplicate scans were collected and averaged, and buffer traces were collected and subsequently subtracted from the protein scans. All scans were integrated to quantify the total fluorescence as a function of denaturant concentration. The data were analyzed using the general purpose nonlinear least-squares fitting program DataFit (Oakdale Engineering) implementing a six-parameter, two-state model (Eftink 1994):

$$F = \frac{F_0 N + (S_N[D]) + (F_O D + (S_D[D])) * e^{-((\Delta G_0 + (m[D]))/RT)}}{1 + e^{-((\Delta G_0 + (m[D]))/RT)}} \quad (1)$$

where the denaturant concentration is given by $[D]$; the native state (0 M denaturant) fluorescence intercept and slope are F_{ON} and S_N, respectively; the denatured state fluorescence intercept and slope are F_{OD} and S_D, respectively; and the free energy of unfolding function intercept and slope are ΔG_O and m, respectively. The ΔG_O and m values describe the linear function of the free energy of unfolding as a function of denaturant under isothermal equilibrium conditions (where ΔG_O is the ΔG value extrapolated to 0 M denaturant, and m is reported as $-d\Delta G/d[D]$). The midpoint of the transition, i.e., the denaturant concentration where $\Delta G = 0$, is defined as C_m. The effect of a given mutation upon the stability of the protein ($\Delta\Delta G$) was calculated using the method of Pace (Pace and Scholtz 1997):

$$\Delta\Delta G = (C_{m\ Wild\ type} - C_{m\ mutant})(m_{Wild\ type} + m_{mutant})/2 \quad (2)$$

where a negative value indicates that the mutation is stabilizing in relationship to the wild-type protein.

Folding kinetic measurements

Denatured protein samples were prepared by overnight dialysis against 20 mM ADA, 100 mM NaCl, 2 mM DTT (pH 6.60) containing either 2.5 M or 3.0 M GuHCl (Blaber et al. 1999).

Initial studies using manual mixing indicated that the relaxation times for the folding process were more appropriate for stopped-flow data collection. All folding kinetic data were collected using a Kintek SF2000 stopped-flow system (Kintek). Folding was initiated by a 1:10 dilution of 40 μM denatured protein into 20 mM ADA, 100 mM NaCl (pH 6.60) with denaturant concentrations varying from 0.25 M GuHCl, in increments of 0.05 M, to the midpoint of denaturation as determined by the above described isothermal equilibrium denaturation measurements. The data collection strategy was designed to span approximately five half-lives, or >97% of the expected fluorescence signal change between the fully denatured and native states.

Unfolding kinetic measurements

Native protein samples were dialyzed against 20 mM ADA 100 mM NaCl, 2 mM DTT (pH 6.60) overnight at 298 K. Unfolding was initiated by a 1:10 dilution of 25 μM protein into 20 mM ADA, 100 mM NaCl (pH 6.60) with concentrations of GuHCl varying between 1.5 M and 5 M. The fluorescence signal associated with protein unfolding was quantified using a Varian Eclipse fluorescence spectrophotometer, with a wavelength of 295 nm for excitation and 350 nm for emission, and maintained at 298 K with a temperature-controlled Peltier cell holder (Varian). The unfolding kinetics exhibited relaxation times that were appropriate for manual mixing techniques. The data collection strategy was designed to span approximately 2–3 half-lives, or >80% of the expected fluorescence signal change between the native and denatured states.

Kinetic analysis

Both folding and unfolding kinetic data were collected in triplicate at each denaturant concentration, with typically six runs per sample and all data being averaged. The kinetic rate constants and amplitudes, as a function of denaturant concentration, were determined from the time-dependent change in fluorescence intensity implementing a single exponential model:

$$I(t) = A * \exp(-k * t) + C \quad (3)$$

where $I(t)$ is the intensity of fluorescent signal at time t, A is the corresponding amplitude, k is the observed rate constant for the reaction, and C is a constant corresponding to the asymptotic signal limit.

Folding and unfolding rate constant data were fit to a global function describing the contribution of both rate constants to the observed kinetics as a function of denaturant ("Chevron" plot) as described by Fersht (1999):

$$\ln(k_{obs}) = \ln(k_{f0} * \exp(m_{kf} * D) + k_{u0} * \exp(m_{ku} * D)) \quad (4)$$

where k_{f0} and k_{u0} are the folding and unfolding rate constants, respectively, extrapolated to 0 M denaturant; m_{kf} and m_{ku} are the slopes of the linear functions relating $\ln(k_f)$ and $\ln(k_u)$, respectively, to denaturant concentration; and D is denaturant concentration.

Crystallization of FGF-1

Purified FGF-1 solutions (~13 mg/mL) were filtered through 0.2-μm filters (Pall Life Sciences) immediately prior to crystallization

trials. X-ray diffraction quality crystals of S50G/V51G grew within 1 wk at RT in 10-µL hanging drops by vapor diffusion against 1-mL reservoirs of 3.0–3.2 M formate and 0.9 M ammonium sulfate in crystallization buffer. V51N and S50E/V51N crystals were obtained within 1 wk at RT in 10-µL hanging drops by vapor diffusion against 3.4–3.6 M formate.

Data collection, molecular replacement, and refinement

X-ray diffraction data were collected using a Rigaku RU-H2R rotating anode X-ray source (Rigaku) equipped with Osmic Blue, or Purple, confocal mirrors (MarUSA) coupled with either a Rigaku R-axis IIc image plate or a MarCCD 165 detector. The crystals were mounted using Hampton Research nylon-mounted cryo-turns and frozen in a stream of nitrogen gas at 100K. Diffraction data were indexed, integrated, and scaled using the DENZO software package (Otwinowski 1993; Otwinowski and Minor 1997). His-tagged wild-type FGF-1 was used as the search model in molecular replacement in each case. Model refinement was carried out with CNS (Brunger et al. 1998) using the maximum likelihood target function. Model building and visualization utilized the O molecular graphics program (Jones et al. 1991).

NMR studies

NMR samples of FGF-1 in 100 mM phosphate buffer, 200 mM ammonium sulfate, and 2 mM DTT (pH 6.0), were labeled uniformly with ^{15}N or ^{13}C using conditions described by Chi et al. (2002). The protein was concentrated to 1 mM, dried by lyophilization, and then resuspended by dissolving in 10% D_2O containing 10 mM phosphate buffer with 90% H_2O. The two- and three-dimensional NMR experiments were performed at 30°C on a 600 MHz Varian UnityPlus spectrometer equipped with waveform generators and pulsed field gradient accessories. Individual spin systems of the wild-type protein were identified via TROSY experiments and then confirmed by 3D HNCACB and CBCA(CO)NH. Individual spin systems of mutant proteins were assigned by HSQC and 3D ^{15}N TOCSY-HSQC experiment.

Acknowledgments

References

Blaber, M., DiSalvo, J., and Thomas, K.A. 1996. X-ray crystal structure of human acidic fibroblast growth factor. *Biochemistry* **35:** 2086–2094.

Blaber, S.I., Culajay, J.F., Khurana, A., and Blaber, M. 1999. Reversible thermal denaturation of human FGF-1 induced by low concentrations of guanidine hydrochloride. *Biophys. J.* **77:** 470–477.

Blanco, F., Ramirez-Alvarado, M., and Serrano, L. 1998. Formation and stability of β hairpin structures in polypeptides. *Curr. Opin. Struct. Biol.* **8:** 107–111.

Blandl, T., Cochran, A.G., and Skelton, N.J. 2003. Turn stability in β-hairpin peptides: Investigation of peptides containing 3:5 type I G1 bulge turns. *Protein Sci.* **12:** 237–247.

Brunger, A.T., Adams, P.D., Clore, G.M., DeLano, W.L., Gros, P., Grosse-Kunstleve, R.W., Jiang, J.-S., Kuszewski, J., Nilges, N., Pannu, N.S., et al. 1998. Crystallography and NMR system (CNS): A new software system for macromolecular structure determination. *Acta Crystallogr. D Biol. Crystallogr.* **54:** 905–921.

Brych, S.R., Blaber, S.I., Logan, T.M., and Blaber, M. 2001. Structure and stability effects of mutations designed to increase the primary sequence symmetry within the core region of a β-trefoil. *Protein Sci.* **10:** 2587–2599.

Chen, P.Y., Lin, C.K., Lee, C.T., Jan, H., and Chan, S.I. 2001. Effects of turn residues in directing the formation of the β-sheet and in the stability of the β-sheet. *Protein Sci.* **10:** 1794–1800.

Chi, Y.H., Kumar, T.K., Chiu, I.M., and Yu, C. 2002. Identification of rare partially unfolded states in equilibrium with the native conformation in an all β-barrel protein. *J. Biol. Chem.* **277:** 34941–34948.

de Alba, E., Jimenez, M.A., and Rico, M. 1997. Turn residue sequence determines β-hairpin conformation in designed peptides. *J. Am. Chem. Soc.* **119:** 175–183.

de Alba, E., Rico, M., and Jimenez, M.A. 1999a. The turn sequence directs β-strand alignment in designed β-hairpins. *Protein Sci.* **8:** 2234–2244.

de Alba, E., Santoro, J., Rico, M., and Jimenez, M.A. 1999b. De novo design of a monomeric three-stranded antiparallel β-sheet. *Protein Sci.* **8:** 854–865.

Eftink, M.R. 1994. The use of fluorescence methods to monitor unfolding transitions in proteins. *Biophys. J.* **66:** 482–501.

Fernandez-Tornero, C., Lozano, R.M., Redondo-Horcajo, M., Gomez, A.M., Lopez, J.C., Quesada, E., Uriel, C., Cuevas, P., Romero, A., and Gimenez-Gallego, G. 2003. Leads for development of new naphthalenesulfonate derivatives with enhanced antiangiogenic activity—Crystal structure of acidic fibroblast growth factor in complex with 5-amino-2-naphthalenesulfonate. *J. Biol. Chem.* **278:** 21774–21781.

Fersht, A.R. 1999. *Kinetics of protein folding.* W.H. Freeman and Co., New York.

Gibbs, A.C., Bjorndahl, T.C., Hodges, R.S., and Wishart, D.S. 2002. Probing the determinants of type II′ β-turn formation in peptides and proteins. *J. Am. Chem. Soc.* **124:** 1203–1209.

Gimenez-Gallego, G., Conn, G., Hatcher, V.B., and Thomas, K.A. 1986. The complete amino acid sequence of human brain-derived acidic fibroblast growth factor. *Biochem. Biophys. Res. Commun.* **128:** 611–617.

Griffiths-Jones, S.R., Maynard, A.J., and Searle, M.S. 1999. Dissecting the stability of a β-hairpin peptide that folds in water: NMR and molecular dynamics analysis of the β-turn and β-strand contributions to folding. *J. Mol. Biol.* **292:** 1051–1069.

Hecht, H.J., Adar, R., Hofmann, B., Bogin, O., Weich, H., and Yayon, A. 2001. Structure of fibroblast growth factor 9 shows a symmetric dimer with unique receptor- and heparin-binding interfaces. *Acta Crystallogr. D Biol. Crystallogr.* **57:** 378–384.

Hutchinson, E.G. and Thornton, J.M. 1994. A revised set of potentials for β-turn formation in proteins. *Protein Sci.* **3:** 2207–2216.

———. 1996. PROMOTIF—A program to identify and analyze structural motifs in proteins. *Protein Sci.* **5:** 212–220.

Jones, T.A., Zou, J.Y., Cowan, S.W., and Kjeldgaard, M. 1991. Improved methods for the building of protein models in electron density maps and the location of errors in these models. *Acta Crystallogr. A* **47:** 110–119.

Kim, J., Blaber, S.I., and Blaber, M. 2002. Alternative type I and I′ turn conformations in the β8/β9 β-hairpin of human acidic fibroblast growth factor. *Protein Sci.* **11:** 459–466.

Kim, J., Brych, S.R., Lee, J., Logan, T.M., and Blaber, M. 2003. Identification of a key structural element for protein folding within β-hairpin turns. *J. Mol. Biol.* **328:** 951–961.

Kortemme, T., Ramirez-Alvarado, M., and Serrano, L. 1998. Design of a 20-amino acid, three-stranded β-sheet protein. *Science* **281:** 253–256.

Kwasigroch, J.M., Chomilier, J., and Mornon, J.P. 1996. A global taxonomy of loops in globular proteins. *J. Mol. Biol.* **259:** 855–872.

Linemeyer, D.L., Menke, J.G., Kelly, L.J., Disalvo, J., Soderman, D., Schaeffer, M.-T., Ortega, S., Gimenez-Gallego, G., and Thomas, K.A. 1990. Disulfide bonds are neither required, present, nor compatible with full activity of human recombinant acidic fibroblast growth factor. *Growth Factors* **3:** 287–298.

Matthews, B., Nicholson, H., and Becktel, W. 1987. Enhanced protein thermostability from site-directed mutations that decrease the entropy of unfolding. *Proc. Natl. Acad. Sci.* **84:** 6663–6667.

Murzin, A.G., Lesk, A.M., and Chothia, C. 1992. β-Trefoil fold. Patterns of structure and sequence in the kunitz inhibitors interleukins-1β and 1α and fibroblast growth factors. *J. Mol. Biol.* **223:** 531–543.

Ogura, K., Nagata, K., Hatanaka, H., Habuchi, H., Kimata, K., Tate, S., Ravera, M.W., Jaye, M., Schlessinger, J., and Inagaki, F. 1999. Solution structure of human acidic fibroblast growth factor and interaction with heparin-derived hexasaccharide. *J. Biomol. NMR* **13:** 11–24.

Olsen, S.K., Garbi, M., Zampieri, N., Eliseenkova, A.V., Ornitz, D.M., Goldfarb, M., and Mohammadi, M. 2003. Fibroblast growth factor (FGF) ho-

mologous factors share structural but not functional homology with FGFs. *J. Biol. Chem.* **278:** 34226–34236.

Orengo, C.A., Jones, D.T., and Thornton, J.M. 1994. Protein superfamilies and domain superfolds. *Nature* **372:** 631–634.

Ortega, S., Schaeffer, M.-T., Soderman, D., DiSalvo, J., Linemeyer, D.L., Gimenez-Gallego, G., and Thomas, K.A. 1991. Conversion of cysteine to serine residues alters the activity, stability, and heparin dependence of acidic fibroblast growth factor. *J. Biol. Chem.* **266:** 5842–5846.

Otwinowski, Z. 1993. Oscillation data reduction program. In *Proceeding of the CCP4 Study Weekend: Data Collection and Processing, 29–30 January 1993* (eds. L. Sawyer et al.), pp. 56–62. SERC Daresbury Laboratory, England.

Otwinowski, Z. and Minor, W. 1997. Processing of x-ray diffraction data collected in oscillation mode. *Methods Enzymol.* **276:** 307–326.

Pace, C.N. and Scholtz, J.M. 1997. Measuring the conformational stability of a protein. In *Protein structure: A practical approach* (ed. T.E. Creighton), pp. 299–321. Oxford University Press, Washington, DC.

Pellegrini, L., Burke, D.F., von Delft, F., Mulloy, B., and Blundell, T.L. 2000. Crystal structure of fibroblast growth factor receptor ectodomain bound to ligand and heparin. *Nature* **407:** 1029–1034.

Pineda-Lucena, A., Jimenez, M.A., Nieto, J.L., Santoro, J., Rico, M., and Gimenez-Gallego, G. 1994. 1H-NMR assignment and solution structure of human acidic fibroblast growth factor activated by inositol hexasulfate. *J. Mol. Biol.* **242:** 81–98.

Ramirez-Alvarado, M., Serrano, L., and Blanco, F.J. 1997. Conformational analysis of peptides corresponding to all the secondary structure elements of protein L B1 domain: Secondary structure propensities are not conserved in proteins with the same fold. *Protein Sci.* **6:** 162–174.

Rotondi, K.S. and Gierasch, L.M. 2003. Local sequence information in cellular retinoic acid binding protein I: Specific residue roles in β-turns. *Biopolymers* **71:** 638–651.

Schenck, H.L. and Gellman, S.H. 1998. Use of a designed triple-stranded antiparallel β-sheet to probe β-sheet cooperativity in aqueous solution. *J. Am. Chem. Soc.* **120:** 4869–4870.

Searle, M.S., Williams, D.H., and Packman, L.C. 1995. A short linear peptide derived from the N-terminal sequence of ubiquitin folds into a water-stable non-native β-hairpin. *Nat. Struct. Biol.* **2:** 999–1006.

Stanger, H.E. and Gellman, S.H. 1998. Rules for antiparallel β-sheet design: D-Pro-Gly is superior to L-Asn-Gly for β-hairpin nucleation. *J. Am. Chem. Soc.* **120:** 4236–4237.

Takano, K., Yamagata, Y., and Yutani, K. 2001. Role of non-glycine residues in left-handed helical conformation for the conformational stability of human lysozyme. *Proteins* **44:** 233–243.